ChemComm

Accepted Manuscript

This article can be cited before page numbers have been issued, to do this please use: M. J. Carnie, C. Charbonnaeu, M. L. Davies, J. Troughton, T. M. Watson, K. Wojciechowski, H. Snaith and D. A. Worsley, *Chem. Commun.*, 2013, DOI: 10.1039/C3CC44177F.

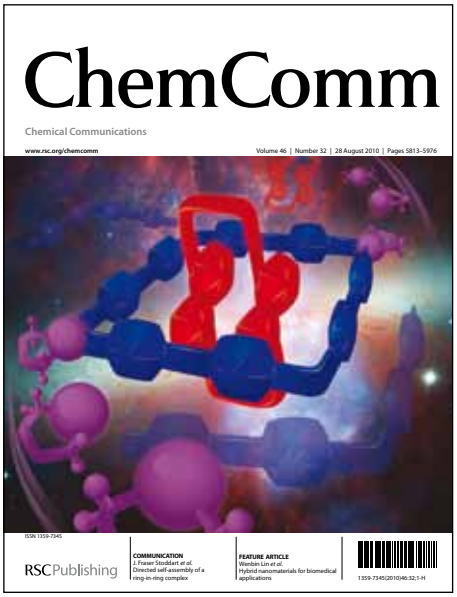

This is an *Accepted Manuscript*, which has been through the RSC Publishing peer review process and has been accepted for publication.

Accepted Manuscripts are published online shortly after acceptance, which is prior to technical editing, formatting and proof reading. This free service from RSC Publishing allows authors to make their results available to the community, in citable form, before publication of the edited article. This *Accepted Manuscript* will be replaced by the edited and formatted *Advance Article* as soon as this is available.

To cite this manuscript please use its permanent Digital Object Identifier (DOI®), which is identical for all formats of publication.

More information about *Accepted Manuscripts* can be found in the **Information for Authors**.

Please note that technical editing may introduce minor changes to the text and/or graphics contained in the manuscript submitted by the author(s) which may alter content, and that the standard **Terms & Conditions** and the **ethical guidelines** that apply to the journal are still applicable. In no event shall the RSC be held responsible for any errors or omissions in these *Accepted Manuscript* manuscripts or any consequences arising from the use of any information contained in them.

Chemical Communications ChemComm

Dynamic Article Links ►
View Article Online
DOI: 10.1039/C3CC44177F

Cite this: DOI: 10.1039/c0xx00000x

www.rsc.org/xxxxxx

Communication

A One-Step Low Temperature Processing Route for Organolead Halide Perovskite Solar Cells

Matthew J. Carnie,[a] Cecile Charbonneau[a] Matthew L. Davies[b] Joel Troughton[a] Trystan M. Watson[a] Konrad Wojciechowski[c], Henry Snaith[c] and David A. Worsley[a]

Received (in XXX, XXX) Xth XXXXXXXXX 20XX, Accepted Xth XXXXXXXXX 20XX
DOI: 10.1039/b000000x

Organolead trihalide perovskite solar cells based upon the co-deposition of a combined Al_2O_3/perovskite layer at T < 110 °C are presented. We report an average PCE = 7.2 % on a non-sintered Al_2O_3 scaffold in devices that have been manufactured from a perovskite precursor containing 5 % wt. Al_2O_3 nanoparticles.

The spectral sensitization of n-type TiO_2 electrodes by polypyridineruthenium (II) complexes was first described by Clark and Sutin in 1977 [1]. This combined with early work on photoelectrochemical cells [2] and dye-sensitization to increase the efficiency of TiO_2 photocatalysis [3], led to the realisation of dye-sensitization for photovoltaic applications and eventually to the work of O' Regan and Grätzel on colloidal, high surface area TiO_2 films. The result was their seminal paper describing high efficiency dye-sensitized solar cells (DSSCs) in 1991 [4]. Further developments of screen printable polymer-organic TiO_2 pastes [5] and high efficiency cells built on metal substrates [6] has led to the realisation that it may be possible to produce DSSCs utilising roll-to-roll processes. Sensitizer and electrolyte developments have recently resulted in DSSCs reaching power conversion efficiencies (PCE) of over 12 % [7].

So far the highest performing devices have utilized dye sensitizers and liquid electrolytes, but alternative configurations have been extensively investigated such as the solid state dye-sensitized solar cell (ss-DSSC), with a solid organic hole transporter [8], and alternative sensitizers such as quantum dots [9]. To date, ss-DSSC power conversion efficiency stands at 7.2 % [10] and the highest recorded for quantum dot devices so far is PCE = 7.0% [11] In 2009, Kojima *et al.* published work on using organometal halide perovskite as sensitizers in liquid electrolyte based devices. They achieved a PCE of 3.8 % with a $CH_3NH_3PbI_3$ perovskite and a V_{OC} of 0.96 V with a $CH_3NH_3Br_3$ perovskite [12]. The realisation that these perovskite materials could be utilised in ss-DSSCs as light harvesters lead to high efficiency devices, whereby a PCE of 9.7 % was achieved [13]. In other work focussing on a mixed halide ($CH_3NH_3PbI_{3-x}Cl_x$) perovskite it was found that electron transport was faster when an alumina scaffold was utilised than when using a TiO_2 scaffold. Higher efficiencies were achieved when using the insulating mesoporous Al_2O_3 scaffold than with a semiconducting mesoporous TiO_2 scaffold/electron-acceptor. A PCE of 10.9 % was achieved with V_{OC} in excess of 1.1 V in a device utilising a sintered alumina scaffold [14]. Caesium tin iodide ($CsSnI_3$) perovskite has also been employed as solid hole conductor in a ss-DSSC with a PCE of 8.5 % [15].

Organolead halide perovskite materials are a promising, low cost, easily synthesised set of materials. They act as light absorber and both electron and hole transporter. Indeed, efficient devices have been made where no organic hole transporter is utilised [16]. All the technologies mentioned so far require a high temperature heating step in order to sinter the TiO_2 or Al_2O_3 nanoparticles. Perhaps from a manufacturing point of view, one of the most promising aspects of the Al_2O_3 based devices is the fact that, as Al_2O_3 is electrically insulating, there is no need to sinter the nanoparticles, as particle interconnectivity will not be as important as it is in TiO_2 based devices where poor particle interconnectivity results in slower electron transport and lower photocurrents [17]. In the work outlined by Lee *et al.* [14], nanoparticles are sintered at 550 °C but this may not be necessary and indeed, low temperature deposition of Al_2O_3 has now been achieved with device performances better than that of devices made with a sintered alumina film [18].

In this work, we propose an alternative method of Al_2O_3/perovskite deposition whereby the two step deposition process can be performed in a single step. The alumina nanoparticles are suspended in the perovskite precursor solution and the Al_2O_3/perovskite layer is co-deposited by spin coating in a single deposition. This is followed by a low temperature heating step at T < 110 °C. The mixed halide perovskite precursor and device manufacturing method outlined by Lee *et al.* [14] have been utilised. Our methodology differs in that instead of depositing a lead halide perovskite precursor solution onto a pre-sintered Al_2O_3 scaffold, we have added Al_2O_3 nanoparticles directly to the perovskite precursor solution. This is followed by a low temperature heating step at T < 110 °C. This has the advantage of combining two manufacturing steps into one and negates the need for a high temperature (550 °C) sintering step. This results in

[a] *SPECIFIC, College of Engineering, Swansea University, Baglan Bay Innovation and Knowledge Centre, Central Avenue, Baglan SA12 7AX, UK. E-mail: d.a.worsley@swansea.ac.uk*
[b] *School of Chemistry, Bangor University, Bangor, Gwynedd UK*
[c] *Photovoltaic and Optoelectronic Device Group, Department of Physics, Oxford University, UK*
† Electronic Supplementary Information (ESI) available: See DOI:10.1039/b000000x/

View Article Online
DOI: 10.1039/C3CC44177F

devices that have a lower embodied energy with a relatively more simple manufacturing process. This may prove to be of great importance to the scale up and manufacture of this technology.

The alumina nanoparticle suspension is obtained from Sigma-Aldrich (20 wt. % in isopropanol). Initial experiments involved adding the alumina suspension directly to the perovskite precursor solution. The resultant Al_2O_3/perovskite precursor solution was non-homogeneous in appearance which we have hypothesised as being caused by mixed solvent/solute incompatibilities, as the perovskite precursor is poorly soluble in isopropanol. Devices made with this Al_2O_3/perovskite solution had low efficiencies. In order for high efficiency devices to be made, it was found that the nanoparticles must be suspended in DMF (N,N-Dimethylformamide). This is achieved *via* solvent exchange in a rotary evaporator whereby equal volumes of the nanoparticle suspension and DMF were put into a round bottom flask. A rotary evaporator is then used to remove the lower boiling point isopropanol, thus leaving the nanoparticles suspended in DMF. The nanoparticle suspension in DMF is then added to the perovskite precursor solution which is also dissolved in DMF. The first devices manufactured, did not perform well and showed evidence of shunting in their IV curves. This was solved by sonication of the nanoparticle suspension for one hour prior to addition to the perovskite precursor solution. This suggests that the shunting could have been caused by nanoparticle aggregation leading to film imhomogeneity and possible contact between the perovskite and the gold counter electrode. Fig. 1 below shows the statistical IV data for all manufactured devices, with varying nanoparticle weight percentages dispersed in the perovskite precursor prior to deposition.

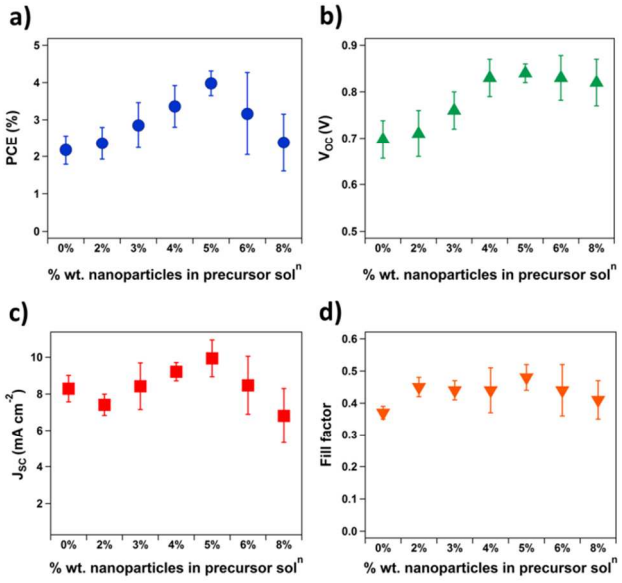

Fig. 1 Statistical IV data showing: a) efficiency (PCE), b) open-circuit voltage (V_{OC}), c) short-circuit current density (J_{SC}) and d) fill-factor (FF) of devices *vs.* the nanoparticle wt. % in the perovskite precursor solution before deposition

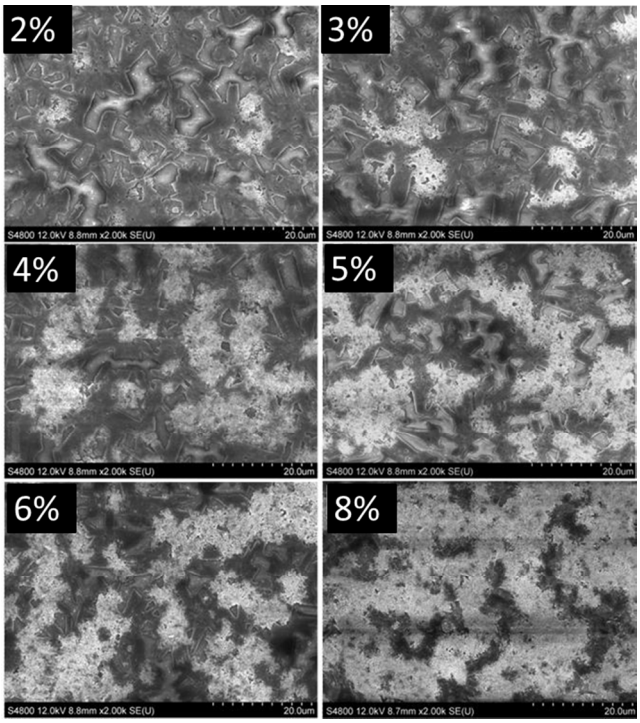

Fig.2 Plan view SEM images of co-deposited Al_2O_3/perovskite films. The wt. % of alumina in the precursor solution prior to spin coating is shown top-left in each SEM micrograph. It can be seen that the co-deposited alumina/perovskite forms a dual-phase structure with alumina rich (lighter shading) and alumina poor (darker shading) areas

It can be seen that device PCE improves as the wt. % is increased from 0 % (a planar junction cell) to 5 %. At higher weight percentages, PCE decreases. Fig. S1† shows the UV-Vis absorbance of co-deposited Al_2O_3/perovskite films, spin coated onto microscope slides, the average Al_2O_3/perovskite film thickness was found to be 400 nm using a profilometer. A cross sectional SEM of the best performing device in this study is shown in Fig. S2†. The absorbance spectra show increasing absorbance with increased particle loading. The increasing PCE (Fig.1) could possibly be due to increased amounts of perovskite crystallizing from the precursor solution with increased nanoparticle wt. %. However, there is also expected to be an increase in light scattering with an increase in nanoparticle wt. % which could account for, at least a proportion of, the absorbance increase. At the highest nanoparticle weight percentages (6 % and 8 % by wt. in the precursor solution), the UV-VIS absorbance continues to increase despite the photovoltaic PCE decreasing at wt. % > 5 %. This decrease in performance may occur due to the dual phase nature that has been observed and is evident in Fig. 2 which shows plan-view SEM images of the same films as in Fig. S1†. EDX analyses of these films shows that there are alumina rich areas (lighter shading, figure 2) and alumina poor areas (darker shading) which could indicate poor wetting of the alumina surface by the perovskite precursor solution. At higher nanoparticle wt. %, electron transport through the perovskite film could be restricted by the large alumina deposits. This is supported by the IV data where devices made with the higher weight percentage precursor solutions show lower photocurrents and fill factors.

View Article Online
DOI: 10.1039/C3CC44177F

To date our most efficient organolead trihalide perovskite devices, incorporating an alumina scaffold, have been manufactured using the low temperature manufacturing method described here. For comparison, a statistical analysis of the 8 most efficient devices made with a sintered (550 °C) Al_2O_3 scaffold has been conducted and the results are summarised in Table S1† where it can be seen that the average PCE = 3.17 % (± 0.88 %). The average device efficiency for the 8 most efficient low T, co-deposited devices is PCE = 3.98 % (± 0.33 %). The improvement in device PCE and improvement in device consistency is in accordance with the recent report by Ball *et al.* in which they have achieved their best device performances with a low temperature Al_2O_3 deposition technique [15].

Following the work presented so far to determine the optimum nanoparticle wt. %, steps have been taken to improve device efficiencies. We have observed that the performance of these devices is sensitive to the relative humidity (RH) in the laboratory at the point of manufacture. When devices are manufactured in an atmosphere of RH < 35 %, improvements in PCE are significant. Indeed, we have recently manufactured our highest efficiency devices, using the low temperature method which is described in the ESI† and by controlling the humidity during manufacture. The average PCE of our ten most recent devices is 7.2 % (± 0.6 %). Fig. 3 shows the IV curve of one such device with PCE = 7.2 %.

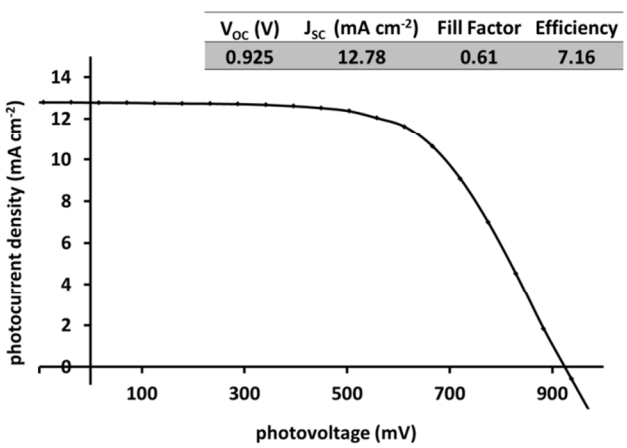

Fig 3. IV curve of the best performing device manufactured so far using the low temperature co-deposition technique.

It can be seen that the fill factor of this device and indeed, of all devices presented in this work, is low. The IV curve above shows evidence of shunting, which could be the source of our comparatively low device efficiencies. This is perhaps as a result of our HTM layer not being optimised (in terms of layer thickness, precursor solution concentration and dopant levels). In fact it should be noted that very little optimisation work has been carried out on these devices. Emphasis has been put on determining the best nanoparticle wt. % in the perovskite precursor and controlling the laboratory humidity during manufacture. Optimisation of the HTM layer is the focus of ongoing work and it is therefore conceivable that devices manufactured in the way described above can match the performance of devices described in [15], especially when the dual phase nature of the co-deposited layer is considered. If it is possible to encourage the perovskite to wet the surface of the nanoparticles more effectively upon crystallization then it may be possible to achieve large improvements in device light harvesting efficiency, which may improve photocurrents. If fill factors can also be improved by HTM optimisation then it is conceivable that high efficiency devices can be manufactured using this low temperature co-deposition technique.

Conclusions

We have shown that it is possible to obtain efficient lead halide based perovskite devices by co-depositing a single Al_2O_3/perovskite layer at low temperatures. We believe this will be of great interest to those working on the development and scale-up manufacture of these devices. Furthermore, we believe that with further optimisation, devices manufactured using this low temperature method can be improved upon and leads to the distinct realisation of highly efficient, low temperature, solid-state devices.

Notes and references

1. W. D. K. Clark and N. Sutin, *J. Am. Chem. Soc.*, 1977, **99**, 4676–4682.
2. A. J. Nozik, *Philos. Trans. R. Soc. Series A.,* 1980, **295**, 453.
3. C. Jaeger, F. Fan, and A. Bard, *J. Am. Chem. Soc.,* 1980, 2592–2598.
4. B. O'Regan, and M. Gratzel, *Nature*, 1991, **353**, 737–740.
5. T. Ma, T. Kida, M. Akiyama, K. Inoue, S. Tsunematsu, K. Yao, H. Noma, and E. Abe, *Electrochem. Comm.*, 2003, **5**, 369–372.
6. S. Ito, N.-L. L. C. Ha, G. Rothenberger, P. Liska, P. Comte, S. M. Zakeeruddin, P. Pechy, M. K. Nazeeruddin, M. Gratzel, P. Péchy, and M. Grätzel, *Chem. Commun.*, 2006, **2006**, 4004–4006.
7. A. Yella, H.-W. W. Lee, H. N. Tsao, C. Yi, A. K. Chandiran, M. K. Nazeeruddin, E. W.-G. G. Diau, C.-Y. Y. Yeh, S. M. Zakeeruddin, and M. Grätzel, *Science*, 2011, **334**, 629–634.
8. U. Bach, D. Lupo, P. Comte, J. E. Moser, F. Weissörtel, J. Salbeck, H. Spreitzer and M. Grätzel, *Nature*, 1998, **395**, 583–585.
9. A. J. Nozik, *Physica E*, 2002, **14**, 115–120.
10. J. Burschka, A. Dualeh, F. Kessler, E. Baranoff, N.-L. Cevey-Ha, C. Yi, M. K. Nazeeruddin, and M. Grätzel, *J. Am. Chem. Soc.,* 2011, 133, 18042–5.
11. A. H. Ip, S. M. Thon, S. Hoogland, O. Voznyy, D. Zhitomirsky, R. Debnath, L. Levina, L. R. Rollny, G. H. Carey, A. Fischer, K. W. Kemp, I. J. Kramer, Z. Ning, A. J. Labelle, K. W. Chou, A. Amassian, and E. H. Sargent, *Nat. Nanotechnol.*, 2012, 7, 577–82.
12. A. Kojima, K. Teshima, Y. Shirai, and T. Miyasaka, *J. Am. Chem. Soc.*, 2009, 131, 6050–1.
13. H.-S. Kim, C.-R. Lee, J.-H. Im, K.-B. Lee, T. Moehl, A. Marchioro, S.-J. Moon, R. Humphry-Baker, J.-H. Yum, J. E. Moser, M. Grätzel, and N.-G. Park, *Sci. Rep.*, 2012, **2**, 1–7.
14. M. M. Lee, J. Teuscher, T. Miyasaka, T. N. Murakami, and H. J. Snaith, *Science*, 2012, **338**, 643–7.
15. I. Chung, B. Lee, J. He, R. P. H. Chang, and M. G. Kanatzidis, *Nature*, 2012, **485**, 486–9.
16. L. Etgar, P. Gao, Z. Xue, Q. Peng, A. K. Chandiran, and B. Liu, 2012, 8–11.
17. M. J. Carnie, C. Charbonneau, P. R. F. Barnes, M. L. Davies, I. Mabbett, T. M. Watson, B. C. O'Regan, and D. A. Worsley, *J. Mater. Chem. A*, 2013, **1**, 2225.
18. J. M. Ball, M. M. Lee, A. Hey, and H. Snaith, *Energ. Environ. Sci.*, 2013.